Azimuthal Anisotropy Distributions in High-Energy Collisions

Li Yan,[1] Jean-Yves Ollitrault,[1] and Arthur M. Poskanzer[2]

[1] *CNRS, URA2306, IPhT, Institut de physique théorique de Saclay, F-91191 Gif-sur-Yvette, France*
[2] *Lawrence Berkeley National Laboratory, Berkeley, California, 94720*

(Dated: August 6, 2014)

Elliptic flow in ultrarelativistic heavy-ion collisions results from the hydrodynamic response to the spatial anisotropy of the initial density profile. A long-standing problem in the interpretation of flow data is that uncertainties in the initial anisotropy are mingled with uncertainties in the response. We argue that the non-Gaussianity of flow fluctuations in small systems can be used to disentangle the initial state from the response. We apply this method to recent measurements of anisotropic flow in Pb+Pb and p+Pb collisions at the LHC. The response coefficient is found to decrease mildly as the system becomes smaller. This mild decrease is consistent with a low value of the ratio of viscosity over entropy.

The large magnitude of elliptic flow, v_2, in relativistic heavy-ion collisions at RHIC [1] and LHC [2] has long been recognized as a signature of hydrodynamic behavior of the strongly-interacting quark-gluon plasma [3]. v_2 is understood as the hydrodynamic response to the initial anisotropy of the initial density profile [4]. However, the magnitude of this anisotropy is poorly constrained theoretically [5, 6]. This uncertainty hinders the extraction of the properties of the quark-gluon plasma from experimental data [7, 8].

The statistical properties of anisotropic flow are now precisely known [9]. The ATLAS collaboration has analyzed the full probability distribution of v_2, v_3 and v_4 in Pb+Pb collisions for several centrality windows [10]. In p+Pb collisions, information is less detailed, but the first moments of the distribution of v_2 have been measured [11]. Our goal is to make use of these measurements to separate the initial state from the response, without assuming any particular model of the initial conditions.

In theory, one can describe the particles emitted from a collision with an underlying probability distribution [12]. Anisotropic flow, v_n, is defined as the $n^{\rm th}$ Fourier coefficient of the azimuthal probability distribution $\mathcal{P}(\varphi)$:

$$V_n = v_n e^{in\Psi_n} \equiv \frac{1}{2\pi}\int_0^{2\pi} \mathcal{P}(\varphi) e^{in\varphi} d\varphi, \qquad (1)$$

where we have used a complex notation [13, 14]. Note that the underlying probability distribution $\mathcal{P}(\varphi)$ and V_n fluctuate event to event, but they are both theoretical quantities which cannot be measured on an event-by-event basis. The particles that are detected in an event represent a finite sample of $\mathcal{P}(\varphi)$, and the measurement of the probability distribution of v_n involves a nontrivial unfolding of statistical fluctuations [10].

We assume that the fluctuations of v_n for $n = 2, 3$ are due to fluctuations of the initial anisotropy ε_n in the corresponding harmonic, defined by [15]

$$\mathcal{E}_n = \varepsilon_n e^{in\Phi_n} \equiv -\frac{\int r^n e^{in\phi} \rho(r,\phi) r {\rm d}r{\rm d}\phi}{\int r^n \rho(r,\phi) r {\rm d}r{\rm d}\phi}. \qquad (2)$$

where $\rho(r,\phi)$ is the energy density near midrapidity shortly after the collision, and (r,ϕ) are polar coordinates in the transverse plane, in a centered coordinate system.

We assume that v_n in a given event is determined by linear response to the initial anisotropy, $v_n = \kappa_n \varepsilon_n$, where κ_n is a response coefficient which does not fluctuate event to event. Event-by-event hydrodynamic calculations [16] show that this is a very good approximation for $n = 2, 3$.[1] Within this approximation, it has already been shown that one can rule out particular models of the initial density using either a combined analysis [18, 19] of elliptic flow and triangular flow [20] data, or the relative magnitude of elliptic flow fluctuations [21–23]. Our goal is to show that one can extract both κ_n and the distribution of ε_n from data without assuming any particular model of the initial state. We make use of the recent observation that the distribution of ε_n is to a large extent universal [24, 25] and can be characterized by two parameters.

Both the magnitude and direction of $\mathcal{E}_n$ fluctuate event to event. The simplest parametrization of these fluctuations is a two-dimensional Gaussian probability distribution which, upon integration over azimuthal angle, yields the Bessel-Gaussian distribution [26]:

$$p(\varepsilon_n) = \frac{\varepsilon_n}{\sigma^2} I_0\left(\frac{\varepsilon_0 \varepsilon_n}{\sigma^2}\right) \exp\left(-\frac{\varepsilon_0^2 + \varepsilon_n^2}{2\sigma^2}\right), \qquad (3)$$

where ε_0 is the mean anisotropy in the reaction plane, which vanishes by symmetry for odd n, and σ is the typical magnitude of eccentricity fluctuations around this mean anisotropy.

In a previous publication [25], we have introduced an alternative parametrization, the Elliptic Power distribution:

$$p(\varepsilon_n) = \frac{\alpha \varepsilon_n}{\pi}(1-\varepsilon_0^2)^{\alpha+\frac{1}{2}} \int_0^{2\pi} \frac{(1-\varepsilon_n^2)^{\alpha-1} d\phi}{(1-\varepsilon_0\varepsilon_n\cos\phi)^{2\alpha+1}}, \qquad (4)$$

where α describes the fluctuations and is approximately proportional to the number of sources in an independent-source model [4]. When $\varepsilon_0 \ll 1$ and $\alpha \gg 1$, Eq. (4)

[1] v_4 is more complicated due to a large nonlinear response [17].

reduces to Eq. (3) with $\sigma \approx 1/\sqrt{2\alpha}$. Its support is the unit disk: it naturally takes into account the condition $|\varepsilon_n| \leq 1$ which follows from the definition, Eq. (2). For this reason, it is a better parametrization than the Bessel-Gaussian, in particular for large anisotropies. Eq. (4) has been shown to fit various initial-state models [25]. Note that ε_0 is not strictly equal to the mean reaction plane eccentricity for the Elliptic Power distribution, but the difference is small for Pb+Pb collisions [25].

When the anisotropy is solely due to fluctuations, $\varepsilon_0 = 0$, the Bessel-Gaussian reduces to a Gaussian distribution:

$$p(\varepsilon_n) = \frac{\varepsilon_n}{\sigma^2} \exp\left(-\frac{\varepsilon_n^2}{2\sigma^2}\right), \tag{5}$$

and the Elliptic Power distribution reduces to the Power distribution [24]:

$$p(\varepsilon_n) = 2\alpha\varepsilon_n(1-\varepsilon_n^2)^{\alpha-1}. \tag{6}$$

Assuming $v_n = \kappa_n\varepsilon_n$, the probability distribution of anisotropic flow, $P(v_n)$, is obtained from the distribution of the initial anisotropy $p(\varepsilon_n)$, by rescaling by the response coefficient κ_n:

$$P(v_n) = \frac{1}{\kappa_n} p\left(\frac{v_n}{\kappa_n}\right). \tag{7}$$

Figure 1 displays the probability distribution of v_2 and v_3 in various centrality windows [10] together with fits using rescaled Bessel-Gaussian and Elliptic Power distributions for v_2, and rescaled Gaussian and Power distributions for v_3. Note that σ and α need not be the same for v_2 and v_3 [25]. Both parametrizations give very good fits to v_2 and v_3 data for the most central bins shown on the figure.[2] As the centrality percentile increases, however, the quality of the Bessel-Gaussian fit becomes increasingly worse, which is reflected by the large χ^2 of the fit, and also clearly seen in the tail of the distribution: it systematically overestimates the distribution for large anisotropies. On the other hand, the Elliptic Power fit is excellent for all centralities. In particular, it falls off more steeply for large v_n, in close agreement with the data.

Note that the Bessel-Gaussian distribution Eq. (3) is scale invariant: rescaling it by κ_n amounts to multiplying both ε_0 and σ by κ_n, so that the fit is degenerate: only the products $\kappa_n\varepsilon_0$ and $\kappa_n\sigma$ can be determined. Therefore the Bessel-Gaussian fit to ATLAS data is in practice a 2-parameter fit for v_2, and a 1-parameter fit for v_3. On the other hand, the Elliptic Power fit is not degenerate because of the cut-off at $\varepsilon_n = 1$ and returns both the response coefficient κ_n and the parameters pertaining to the initial state, namely α and ε_0 (for v_2). The fit is still strongly correlated in the sense that the combinations $\kappa_n/\sqrt{\alpha}$ and $\kappa_n\varepsilon_0$ (for v_2) have much smaller errors than each individual parameter.

Our ability to separate the response from the initial eccentricity thus lies in the difference between the Bessel-Gaussian and the Elliptic Power fits, that is, in the non-Gaussianity of flow fluctuations. Since the difference is small, errors must be carefully evaluated. They can be divided into experimental errors and theoretical errors. The two sources of theoretical errors are deviations from linear eccentricity scaling, and deviations of the distribution of the initial anisotropy from the Elliptic Power ansatz.

We first discuss experimental errors. The ATLAS collaboration reports the statistical error, the systematic error on the mean $\langle v_n\rangle$, and the systematic error on the relative standard deviation $\sigma_{v_n}/\langle v_n\rangle$. The first systematic error is an error on the scale of the distribution, while the second is an error on its shape. The error on the scale directly translates into an error of the response coefficient κ_n, of the same relative magnitude. Since our analysis uses the deviations from a Gaussian shape, the dominant source of error is —by far— the error on the shape. In order to estimate the corresponding error on our fit parameters, we distort the distribution of v_n in such a way that the mean $\langle v_n\rangle$ is unchanged, and $\sigma_{v_n}/\langle v_n\rangle$ is increased or decreased by the experimental uncertainty.

Figure 2 (a) displays the value of the response coefficients κ_2 and κ_3 as a function of the centrality percentile. They are smaller than unity, with $\kappa_3 < \kappa_2$, in line with expectations from hydrodynamic calculations [16], and decrease mildly as a function of the centrality percentile, which is the general behavior expected from viscous corrections to local equilibrium [30, 31]. We estimate that the low-p_T cut of ATLAS at 0.5 GeV increases κ_2 by a factor $1.4-1.5$. The systematic error for κ_3 is very large and therefore not shown: for most bins, the upper error bar goes all the way to infinity. Now, if one takes the limit $\kappa_3 \to \infty$ while keeping the rms v_3 constant, α in Eq. (6) also goes to infinity and the Power distribution reduces to a Gaussian distribution Eq. (5). Therefore the ATLAS v_3 distributions are compatible with Gaussians within systematic errors.

For p+Pb collisions, the full distribution of v_2 has not been measured, but only its first cumulants [32, 33] $v_2\{2\}$ and $v_2\{4\}$ [11, 34, 35]. Assuming linear response to the initial eccentricity, each measured cumulant is proportional to the corresponding cumulant of the initial eccentricity [36], $v_2\{k\} = \kappa_2\varepsilon_2\{k\}$, for $k = 2, 4, 6...$ The eccentricity in p+Pb collisions is solely due to fluctuations [37, 38], therefore Eqs. (5) and (6) apply. While cumulants of order 4 and higher vanish for the Gaussian distribution Eq. (5), the Power distribution Eq. (6) always gives $\varepsilon_n\{4\} > 0$ [24]. We again use this non-Gaussianity to disentangle the initial state from the response: We extract α from the measured ratio $v_n\{4\}/v_n\{2\} \simeq \varepsilon_n\{4\}/\varepsilon_n\{2\} = (1+\frac{\alpha}{2})^{-1/4}$ [24]. The rms

[2] The fits do not converge below 10% (20%) centrality for v_2 (v_3), which reflects the fact that the distribution is very close to Bessel-Gaussian (Gaussian).

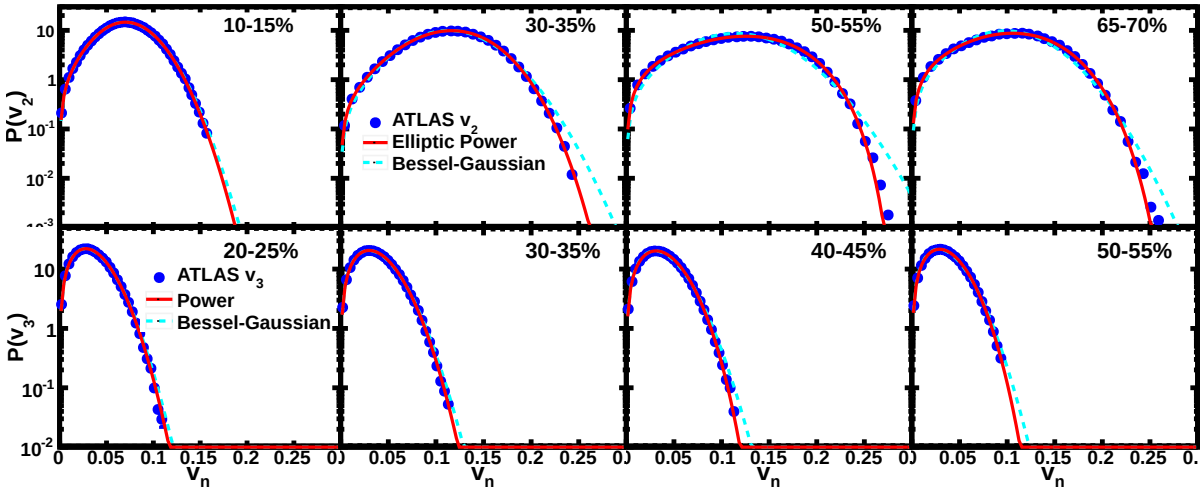

FIG. 1. (Color online) Distribution of v_2 (top) and v_3 (bottom) in various centrality windows. Symbols: ATLAS data [10] for Pb+Pb collisions at $\sqrt{s_{NN}} = 2.76$ TeV. For v_2, fits are rescaled Elliptic Power Eq. (4) (full lines) and Bessel-Gaussian distributions Eq. (3) (dashed lines). For v_3, fits are rescaled Power Eq. (6) (full lines) and Bessel-Gaussian distributions with $\varepsilon_0 = 0$ Eq. (5) (dashed lines).

anisotropy is then obtained as $\varepsilon_n\{2\} = 1/\sqrt{1+\alpha}$ [24]. One finally obtains for the Power distribution:

$$\kappa_n = \frac{v_n\{2\}}{\varepsilon_n\{2\}} = v_n\{2\}\sqrt{2\left(\frac{v_n\{2\}}{v_n\{4\}}\right)^4 - 1}. \qquad (8)$$

The values of κ_2 extracted from CMS p+Pb data [11] using this equation are also displayed in Fig. 2 (a).[3] We multiply them by a factor 1.19 to correct for the different low-p_T cut (0.3 GeV/c) assuming a linear dependence of v_2 on p_T. We plot p+Pb data at the equivalent centralities, determined according to the number of charged tracks [11]. General arguments have been put forward which suggest that the hydrodynamic response should be identical for p+Pb and Pb+Pb at the same equivalent centrality [39]. Once rescaled, the p+Pb slope is in line with Pb+Pb results, albeit somewhat steeper.

Note that the fit parameters can also be obtained from cumulants for v_3 in Pb+Pb collisions using Eq. (8). For v_2, there is a third parameter ε_0, therefore one needs a third cumulant $v_2\{6\}$. α and ε_0, which control the shape of the distribution and its non-Gaussian features, can be extracted from the ratios $v_2\{6\}/v_2\{4\}$ and $v_2\{4\}/v_2\{2\}$ using the Elliptic Power distribution (Eq. (A5) of Ref. [25]). Note that while the Bessel-Gaussian Eq. (3) gives $\varepsilon_n\{4\} = \varepsilon_n\{6\} = \varepsilon_0$ [40], the Elliptic Power distribution always gives $\varepsilon_n\{6\} < \varepsilon_n\{4\}$. We have checked that α and ε_0 thus extracted from cumulant ratios are essentially identical to those obtained by fitting the distribution of v_2. This approach has the advantage that cumulants can be analyzed without any unfolding procedure [33] but $v_2\{2\}$ may suffer from non-flow effects.

We now briefly discuss the effect of the first theoretical error, namely, deviations from linear eccentricity scaling of anisotropic flow. A quantitative measure of the accuracy of eccentricity scaling is the Pearson correlation coefficient r_n between V_n and $\mathcal{E}_n$, defined as

$$r_n \equiv \frac{\langle V_n \mathcal{E}_n^* \rangle}{\sqrt{\langle |V_n|^2 \rangle \langle |\mathcal{E}_n|^2 \rangle}}, \qquad (9)$$

where angular brackets denote an average value over events in a centrality class. Our analysis assumes the maximum correlation, $|r_n| = 1$. Event-by-event hydrodynamic calculations show that there are small deviations from eccentricity scaling [41]. In order to estimate their magnitude, we decompose the flow as $V_n = \kappa_n \mathcal{E}_n + X_n$, where X_n is a complex Gaussian noise, uncorrelated with the initial eccentricity $\mathcal{E}_n$. Then the numerator of Eq. (9) is unchanged, while the denominator is increased by the noise. For example we find that a decrease of $|r_2|$ by 1% results in an decrease of the extracted κ_2 by 8% in the 30-40% centrality range. Ideal event-by-event hydrodynamic calculations [17] give $|r_2| \sim 0.95$ for elliptic flow. However, the correlation between v_n and ε_n has been shown to be significantly larger in viscous hydrodynamics [16], and a value $|r_2| = 0.99$ seems reasonable, but there is to date no quantitative estimate of $|r_2|$ as defined in Eq. (9).

We now compare our result for κ_n with hydrodynamic calculations. In ideal hydrodynamics, scale invariance implies that the response coefficient κ_n is independent of the system size, i.e., independent of centrality. Deviations from thermal equilibrium generally result in a

[3] We cannot use ATLAS data [34], because $v_2\{2\}$ has no rapidity gap and is therefore biased by nonflow effects. ALICE [35] has a smaller rapidity gap than CMS but the resulting values of κ_2 (not shown) are significantly larger.

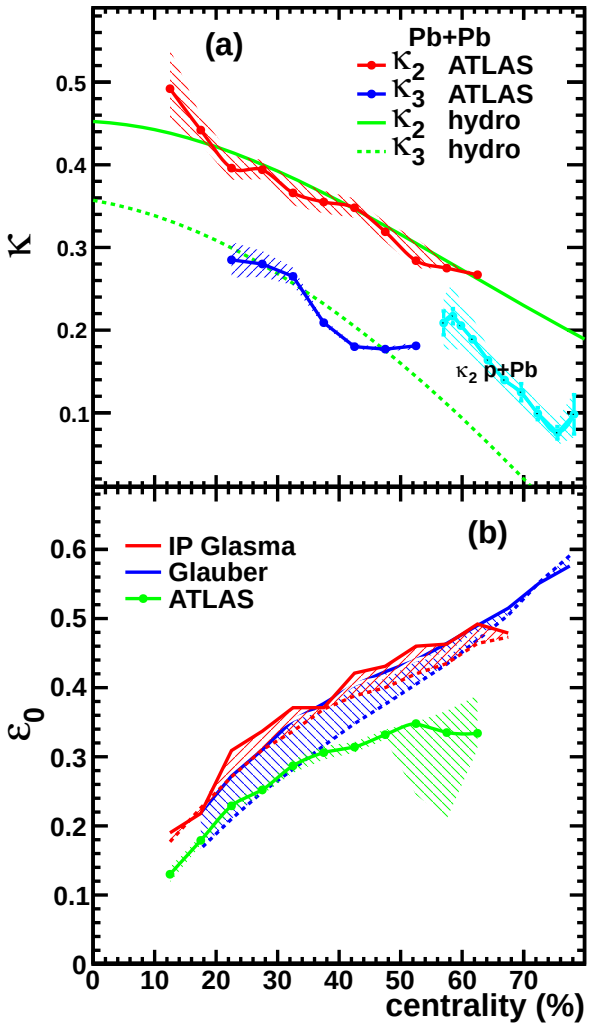

FIG. 2. (Color online) (a) Response coefficients κ_2 and κ_3 versus centrality. Symbols: results from the fits to ATLAS Pb+Pb data [10] and to CMS p+Pb data [11]. For κ_2, systematic and statistical experimental errors are added in quadrature. For κ_3, only the statistical error is shown. Lines are results of a viscous hydrodynamic calculation with $\eta/s = 0.18$ for κ_2, and $\eta/s = 0.14$ for κ_3. (b) ε_0 versus centrality. Symbols: results from the fits to ATLAS v_2 data. The experimental error is shown as a shaded band. Predictions from the Monte-Carlo Glauber [27] and IP-Glasma [28, 29] models are also shown as shaded bands.

reduction of the flow which is stronger for peripheral collisions [30, 31]. In a hydrodynamic calculation [8], such deviations are due to the shear viscosity [7] and, to a lesser extent, to the freeze-out procedure at the end of the hydrodynamic expansion. Therefore the dependence of κ_n on centrality in Fig. 2 (a) can be used to estimate the shear viscosity over entropy ratio η/s of the quark-gluon plasma. We use the same hydrodynamic code as in Ref. [42] to estimate κ_n. The resulting values are significantly smaller than in Fig. 2 (a). Since, however, deviations from eccentricity scaling may reduce κ_n without altering significantly its centrality dependence, we compensate for this effect by multiplying our hydrodynamic result by a constant, and we tune the viscosity so as to match the centrality dependence of κ_n. The κ_2 line in Fig. 2 (a) is obtained with $\eta/s = 0.18$ and a global multiplicative factor of 1.7. The κ_3 line is obtained with $\eta/s = 0.14$ and a global multiplicative factor of 2. These multiplicative factors mean that the values of κ_n in Fig. 2 (a) are larger than expected from hydrodynamics, even if one takes into account the increase due to the ATLAS p_T cut. These extracted values of η/s are consistent with those reported in the literature [8], using specific models of the initial state.

The other parameters of the fit to v_n distributions, namely, α and ε_0, characterize the distribution of the initial anisotropy. Figure 2 (b) displays ε_0 as a function of the collision centrality. ε_0 increases smoothly with the centrality percentile: extrapolation to the most central collisions (where the fit does not converge) gives $\varepsilon_0 = 0$, as required by azimuthal symmetry.

Figure 2 (b) also displays comparisons with the Glauber [27, 43, 44] and IP-Glasma [28, 29] models, shown as shaded bands. The bands correspond to the second theoretical uncertainty, namely, the fact that the Elliptic Power distribution does not exactly fit the distribution of ε_2 for that particular model. Specifically, the dashed line (lower limit of the band) is the value of ε_0 returned by a 2-parameter Elliptic Power fit to the distribution of ε_2. The full line (upper limit of the band) is the value of ε_0 that the fit to the v_2 distribution would return if $v_2 \propto \varepsilon_2$, with ε_2 given by that model. ATLAS data are below the full lines for both models. Note that a lower value of ε_0 corresponds to a larger value of κ_2. Slight deviations from eccentricity scaling would make κ_2 smaller and ε_0 larger, thus improving compatibility with both hydrodynamics and existing initial-state models.

We have shown that a rescaled Elliptic Power distribution fits the measured distributions of elliptic and triangular flows in Pb+Pb collisions at the LHC. These distributions become increasingly non-Gaussian as the anisotropy increases. We have used this non-Gaussianity to disentangle for the first time the initial anisotropy from the response, without assuming any particular model of initial conditions. This is another aspect of the analogy between heavy-ion physics and cosmology [45, 46], where initial quantum fluctuations give rise to correlations, and the non-Gaussian statistics of these correlations can be used to unravel the properties of the initial state [47–49]. The non-Gaussianity is stronger for smaller systems, which is an incentive to analyze flow in smaller collision systems. We have found that the hydrodynamic response to ellipticity decreases mildly with centrality percentage. A similar slope is found for p+Pb collisions. Comparison with hydrodynamic calculations supports a low value of the viscosity over entropy ratio.

ACKNOWLEDGMENTS

We thank M. Luzum and S. Voloshin for extensive discussions and suggestions. In particular, we thank S. Voloshin for useful comments on the manuscript. JYO thanks the MIT LNS for hospitality. LY is funded by the European Research Council under the Advanced Investigator Grant ERC-AD-267258. AMP was supported by the Director, Office of Science, of the U.S. Department of Energy.

[1] K. H. Ackermann *et al.* [STAR Collaboration], Phys. Rev. Lett. **86**, 402 (2001) [nucl-ex/0009011].

[2] KAamodt *et al.* [ALICE Collaboration], Phys. Rev. Lett. **105**, 252302 (2010) [arXiv:1011.3914 [nucl-ex]].

[3] P. F. Kolb and U. W. Heinz, In 'Hwa, R.C. (ed.) et al.: Quark gluon plasma" 634-714 [nucl-th/0305084].

[4] J. -Y. Ollitrault, Phys. Rev. D **46**, 229 (1992).

[5] T. Hirano, U. W. Heinz, D. Kharzeev, R. Lacey and Y. Nara, Phys. Lett. B **636**, 299 (2006) [nucl-th/0511046].

[6] T. Lappi and R. Venugopalan, Phys. Rev. C **74**, 054905 (2006) [nucl-th/0609021].

[7] M. Luzum and P. Romatschke, Phys. Rev. C **78**, 034915 (2008) [Erratum-ibid. C **79**, 039903 (2009)] [arXiv:0804.4015 [nucl-th]].

[8] U. Heinz and R. Snellings, Ann. Rev. Nucl. Part. Sci. **63**, 123 (2013) [arXiv:1301.2826 [nucl-th]].

[9] J. Jia, arXiv:1407.6057 [nucl-ex].

[10] G. Aad *et al.* [ATLAS Collaboration], JHEP **1311**, 183 (2013) [arXiv:1305.2942 [hep-ex]].

[11] S. Chatrchyan *et al.* [CMS Collaboration], Phys. Lett. B **724**, 213 (2013) [arXiv:1305.0609 [nucl-ex]].

[12] M. Luzum and H. Petersen, J. Phys. G **41**, 063102 (2014) [arXiv:1312.5503 [nucl-th]].

[13] J. -Y. Ollitrault and F. G. Gardim, Nucl. Phys. A **904-905**, 75c (2013) [arXiv:1210.8345 [nucl-th]].

[14] D. Teaney and L. Yan, arXiv:1312.3689 [nucl-th].

[15] D. Teaney and L. Yan, Phys. Rev. C **83**, 064904 (2011) [arXiv:1010.1876 [nucl-th]].

[16] H. Niemi, G. S. Denicol, H. Holopainen and P. Huovinen, Phys. Rev. C **87**, 054901 (2013) [arXiv:1212.1008 [nucl-th]].

[17] F. G. Gardim, F. Grassi, M. Luzum and J. -Y. Ollitrault, Phys. Rev. C **85**, 024908 (2012) [arXiv:1111.6538 [nucl-th]].

[18] B. H. Alver, C. Gombeaud, M. Luzum and J. -Y. Ollitrault, Phys. Rev. C **82**, 034913 (2010) [arXiv:1007.5469 [nucl-th]].

[19] E. Retinskaya, M. Luzum and J. -Y. Ollitrault, Phys. Rev. C **89**, 014902 (2014) [arXiv:1311.5339 [nucl-th]].

[20] B. Alver and G. Roland, Phys. Rev. C **81**, 054905 (2010) [Erratum-ibid. C **82**, 039903 (2010)] [arXiv:1003.0194 [nucl-th]].

[21] B. Alver *et al.* [PHOBOS Collaboration], Phys. Rev. Lett. **98**, 242302 (2007) [nucl-ex/0610037].

[22] B. Alver *et al.* [PHOBOS Collaboration], Phys. Rev. C **81**, 034915 (2010) [arXiv:1002.0534 [nucl-ex]].

[23] T. Renk and H. Niemi, Phys. Rev. C **89**, 064907 (2014) [arXiv:1401.2069 [nucl-th]].

[24] L. Yan and J. -Y. Ollitrault, Phys. Rev. Lett. **112**, 082301 (2014) [arXiv:1312.6555 [nucl-th]].

[25] L. Yan, J. -Y. Ollitrault and A. M. Poskanzer, arXiv:1405.6595 [nucl-th].

[26] S. A. Voloshin, A. M. Poskanzer, A. Tang and G. Wang, Phys. Lett. B **659**, 537 (2008) [arXiv:0708.0800 [nucl-th]].

[27] B. Alver, M. Baker, C. Loizides and P. Steinberg, arXiv:0805.4411 [nucl-ex].

[28] B. Schenke, P. Tribedy and R. Venugopalan, Phys. Rev. C **86**, 034908 (2012) [arXiv:1206.6805 [hep-ph]].

[29] B. Schenke, P. Tribedy and R. Venugopalan, Nucl. Phys. A **926**, 102 (2014) [arXiv:1312.5588 [hep-ph]].

[30] S. A. Voloshin and A. M. Poskanzer, Phys. Lett. B **474**, 27 (2000) [nucl-th/9906075].

[31] H. -J. Drescher, A. Dumitru, C. Gombeaud and J. -Y. Ollitrault, Phys. Rev. C **76**, 024905 (2007) [arXiv:0704.3553 [nucl-th]].

[32] N. Borghini, P. M. Dinh and J. -Y. Ollitrault, Phys. Rev. C **64**, 054901 (2001) [nucl-th/0105040].

[33] A. Bilandzic, R. Snellings and S. Voloshin, Phys. Rev. C **83**, 044913 (2011) [arXiv:1010.0233 [nucl-ex]].

[34] G. Aad *et al.* [ATLAS Collaboration], Phys. Lett. B **725**, 60 (2013) [arXiv:1303.2084 [hep-ex]].

[35] B. B. Abelev *et al.* [ALICE Collaboration], arXiv:1406.2474 [nucl-ex].

[36] M. Miller and R. Snellings, nucl-ex/0312008.

[37] P. Bozek, Phys. Rev. C **85**, 014911 (2012) [arXiv:1112.0915 [hep-ph]].

[38] P. Bozek and W. Broniowski, Phys. Lett. B **718**, 1557 (2013) [arXiv:1211.0845 [nucl-th]].

[39] G. Basar and D. Teaney, arXiv:1312.6770 [nucl-th].

[40] A. Bzdak, P. Bozek and L. McLerran, Nucl. Phys. A **927**, 15 (2014) [arXiv:1311.7325 [hep-ph]].

[41] H. Holopainen, H. Niemi and K. J. Eskola, Phys. Rev. C **83**, 034901 (2011) [arXiv:1007.0368 [hep-ph]].

[42] D. Teaney and L. Yan, Phys. Rev. C **86**, 044908 (2012) [arXiv:1206.1905 [nucl-th]].

[43] M. L. Miller, K. Reygers, S. J. Sanders and P. Steinberg, Ann. Rev. Nucl. Part. Sci. **57**, 205 (2007) [nucl-ex/0701025].

[44] W. Broniowski, P. Bozek and M. Rybczynski, Phys. Rev. C **76**, 054905 (2007) [arXiv:0706.4266 [nucl-th]].

[45] A. P. Mishra, R. K. Mohapatra, P. S. Saumia and A. M. Srivastava, Phys. Rev. C **77**, 064902 (2008) [arXiv:0711.1323 [hep-ph]].

[46] K. Dusling, F. Gelis and R. Venugopalan, Nucl. Phys. A **872**, 161 (2011) [arXiv:1106.3927 [nucl-th]].

[47] J. M. Maldacena, JHEP **0305**, 013 (2003) [astro-ph/0210603].

[48] N. Bartolo, E. Komatsu, S. Matarrese and A. Riotto, Phys. Rept. **402**, 103 (2004) [astro-ph/0406398].

[49] P. A. R. Ade *et al.* [Planck Collaboration], arXiv:1303.5084 [astro-ph.CO].